Author(s): Liimatainen, Ville & Shah, Ali & Johansson, Leena-Sisko & Houbenov, Nikolay & Zhou, Quan

Title: Maskless, High-Precision, Persistent, and Extreme Wetting-Contrast Patterning in an Environmental Scanning Electron Microscope

Year: 2016

Version: Pre-print

Please cite the original version:

Liimatainen, Ville & Shah, Ali & Johansson, Leena-Sisko & Houbenov, Nikolay & Zhou, Quan. 2016. Maskless, High-Precision, Persistent, and Extreme Wetting-Contrast Patterning in an Environmental Scanning Electron Microscope. Small. 18. 1613-6810 (printed). DOI: 10.1002/smll.201503127.

DOI: 10.1002/((please add manuscript number))
Article type: Communication

Maskless, High-Precision, Persistent and Extreme Wetting-Contrast Patterning in an Environmental Scanning Electron Microscope

*Ville Liimatainen, Ali Shah, Leena-Sisko Johansson, and Quan Zhou**

V. Liimatainen, Prof. Q. Zhou
Department of Electrical Engineering and Automation, School of Electrical Engineering, Aalto University
Otaniementie 17, Espoo 02150, Finland
E-mail: quan.zhou@aalto.fi

A. Shah
Department of Micro- and Nanosciences, School of Electrical Engineering, Aalto University

Dr. L-S. Johansson
Department of Forest Products Technology, School of Chemical Technology, Aalto University

Keywords: wettability patterning, electron beam modification, ESEM, superhydrophobicity, superhydrophilicity

Since the past decade, micro- and nanopatterns with high wetting contrast for water have been reported on natural[1,2] and man-made[3,4] surfaces. Such patterns have found uses in a diverse set of applications, including water collection from humid air mimicking desert beetles;[5] enhancing boiling heat transfer;[6] microelectromechanical systems (MEMS) assembly using surface tension-driven self-alignment;[7] arranging nanostructures in ordered arrays[8] for

nanophotonic devices e.g. antennas, filters and optical processing circuits;[9] transport of both droplets[10] and liquid flows[11] for lab-on-a-chip devices; and solving cross-contamination and cell migration problems in ultrahigh-density living cell microarrays.[12] Many highly successful methods utilizing well-developed technologies have been employed to produce those micro and nanoscale wetting features, from conventional photolithographic methods, laser interference lithography,[13,14] electron beam lithography (EBL),[15,16] to near-field scanning optical microscopy (NSOM),[17,18] microcontact printing (μCP)[19,20] and pulsed laser beams;[21,22] however, these techniques also have their limitations. For example, in conventional photolithography, sub-μm resolution requires expensive equipment and the wet processing steps may damage the often delicate surface structure of superhydrophobic substrates; laser interference lithography can only produce features in the shape of a few types of interference patterns; microcontact printing techniques use a stamping process that is challenging to apply on rough surfaces;[23] focused, pulsed laser beams have a resolution of few μm, limited by the beam spot size; and specific, photo- or electron sensitive materials are required for NSOM and EBL. The pursuit for an effective method of fabricating high-resolution wetting patterns with extreme wetting contrast is still ongoing.

One potential solution is direct electron beam writing, where the beam modifies the surface directly without any pattern-transferring layer or further processing steps. In previous works, the effect of electron beams on surface wetting properties has been studied; e.g. high-energy electron beams (> 500 keV) can tune the wettability of poly(ethylene terephthalate) (PET) films,[24] poly-l-lactic acid (PLLA),[25] rubber[26] and textile fabrics,[27] where the maximum changes in water contact angles varied from 15° to 32°; and low-energy electron beams (< 0.5 keV) [28,29] can increase the water contact angle by 71° on a silicon dioxide surface, and by 25° on a zinc oxide nanomaterial. In the aforementioned works, electron beam has not been controlled to produce wetting patterns in specific shapes on the surface.

In this paper, we propose a direct writing method for making high-precision, persistent wetting patterns with 152° contact angle contrast on a superhydrophobic substrate using programmable scanning beam in an environmental scanning electron microscope (ESEM). The wetting patterns are produced when the electron beam hits the surface through water vapor and residual nitrogen, creating a plasma that interacts with the surface, rendering it superhydrophilic according to the scanned pattern. The concept is depicted in **Figure 1**a. The surface we use is so-called black silicon with a fluorinated polymer coating, however, we have achieved similar effects on other materials as well. We have fabricated various patterns ranging from μm to mm in size, and demonstrated the wetting contrast by contact angle measurements and condensation tests in ambient air. Our method is maskless and programmable, and the patterns persist over a long period of time, even after one year.

The superhydrophobic surface we mainly focus on is black silicon coated with 200 nm of a poly(p-xylylene) polymer, parylene-C, and then fluorinated in SF_6 plasma. Black silicon, also known as silicon nanograss, is one of the nanostructured materials that have been actively employed in wetting applications,[30–35] because it is easy to render superhydrophobic by applying just one layer of coating[36] due to the high surface roughness. Parylene is a family of biocompatible polymers with good barrier properties, and controllable wettability and adhesion.[37] Morphology of the surface before and after the polymer coating is shown in the SEM micrographs in Figure 1b-c. The coated surface has an initial static contact angle of 130°, which is increased by fluorination in SF_6 plasma. The advancing and receding contact angles after fluorination are 162° and 134°, respectively.

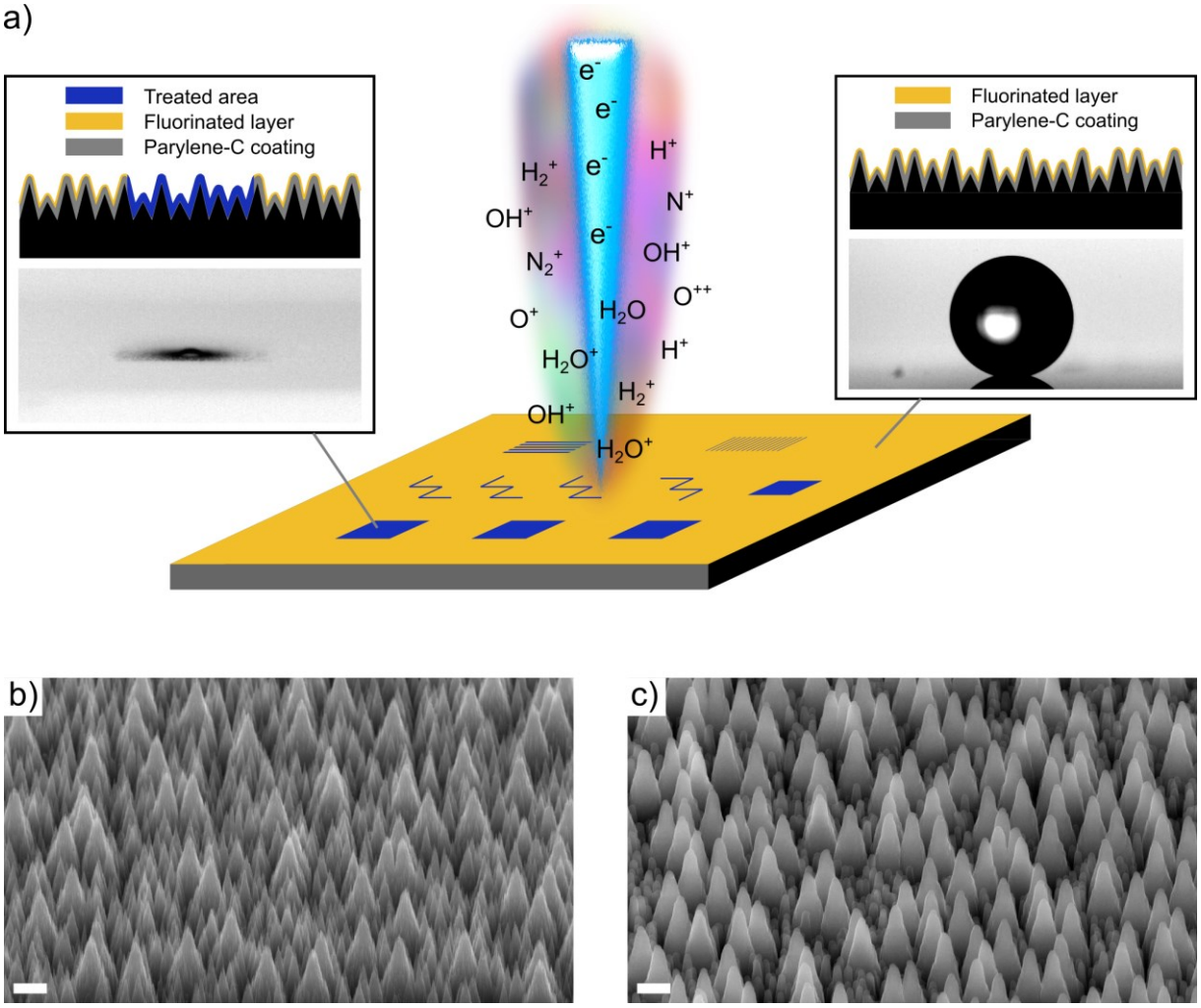

Figure 1. Concept of the direct electron beam writing and morphogoly of the black silicon substrate. a) Concept of extreme wetting contrast micropatterning in ESEM. The electron beam ionizes water vapor and nitrogen present in the chamber, and the resulting plasma interacts with the surface within the scanned pattern, turning it from superhydrophobic to superhydrophilic. b) SEM micrograph of the black silicon substrate before coating. c) SEM micrograph of the black silicon substrate after 200 nm parylene-C coating and fluorination in SF_6 plasma. Scale bars 2 µm.

To create superhydrophilic patterns on the superhydrophobic substrate in the ESEM, a 30 kV acceleration voltage and 5 nA beam current at 4.5 mm working distance were used, with exposure duration of 5 – 15 ms μm^{-2}, corresponding to a charge dose of 2.5 – 7.5 mC cm^{-2}. Advancing and receding contact angles on a 900 × 675 μm^2 treated area were measured to be 10° and 0°, respectively. The wetting contrast was also validated by shooting nanoliter-sized droplets at the surface, where the droplets either bounce away on impact on the non-treated background or immediately spread to cover the whole treated area within 100 ms (Movie S1,

Supporting Information). Reference tests with identical treatment parameters were carried out both in high vacuum and with pure nitrogen as imaging gas, but no noticeable change was observed in the wetting properties.

Water condensation tests in ambient air were carried out to study the short-term persistence of the fabricated wetting patterns. The tests show water emerging as a film on the treated superhydrophilic areas, whereas dropwise condensation is observed on the non-treated superhydrophobic background. The optical micrograph sequence in **Figure 2**a-e shows different phases of the condensation process (see also Movie S2, Supporting Information). After each condensation test, the sample was heated to remove the water. Several condensation-evaporation cycles were carried out, and the wetting behavior of the patterns remains highly repeatable. Condensation tests carried out more than one year after the treatment showed no change in the wetting contrast, verifying the long-term persistence of the patterns.

In the absence of water, the treated areas cannot be visually distinguished under optical microscope. However, the areas shine brightly when illuminated with UV light (320 – 450 nm range), as shown in Figure 2f. The wetting properties of the treated areas show no sign of degradation after 5 min exposure to UV light based on additional condensation tests, but the non-treated background starts to lose the superhydrophobicity during continued UV exposure. This effect can be attributed to the photooxidation of parylene-C, which is known to reduce water contact angle on the surface.[38] To avoid potential influence of UV exposure on the results, the UV visualization was done only after the condensation tests and contact angle measurements, or on separate samples.

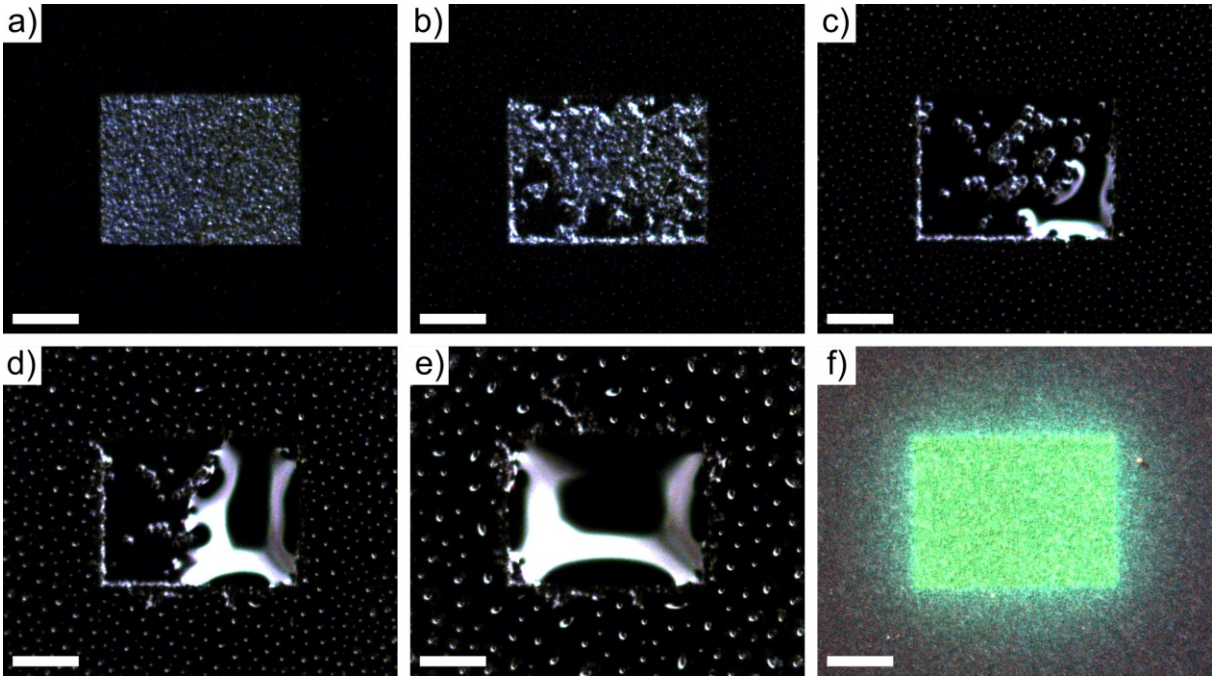

Figure 2. Condensation in ambient air on a treated area, and UV-induced glowing. a-e) Dark field optical micrograph sequence of water condensation in ambient atmosphere on a 300 × 225 μm^2 rectangular area treated with electron beam in an ESEM; f) glow of the treated area when illuminated by UV-light (320 – 450 nm). Scale bars 100 μm.

In addition to area patterns, we programmed the scanning speed and trajectory to produce line segments and examine the possibility of creating small wetting features using the proposed method. Water condensation on various line patterns are shown in **Figure 3**. For the patterns in Figure 3a and c, water condensing on the lines was collected to growing droplets along the treated parts. For the pattern in Figure 3b, the larger, continuous area at the end of the line collected the condensing water. When writing straight lines, two different programming approaches were used: either the sample stage or the beam was moved. In the former case, linewidth could be freely chosen by adjusting the scanning window size, while in the latter case it was determined by the beam spot size.

To explore the lower limit of the wetting pattern resolution, ten straight lines were produced by moving the beam over each line for progressively decreasing duration. The first line was produced in 1 s, and the scanning duration was reduced in 0.1 s steps down to 0.1 s for the last

line. The lines were visualized in an inverted optical microscope (Figure 3d), where the sample was illuminated with blue light in the 450µm – 489µm wavelength range. The linewidth starts from around 2 µm and decreases with decreasing scanning duration. The average width of the last line is estimated around 1 µm where sub-µm segments can be observed. This approaches the limit where the treated area can be considered homogeneous for the purposes of wetting and condensation, because the surface has a feature size of approximately 1 µm (Figure 1c).

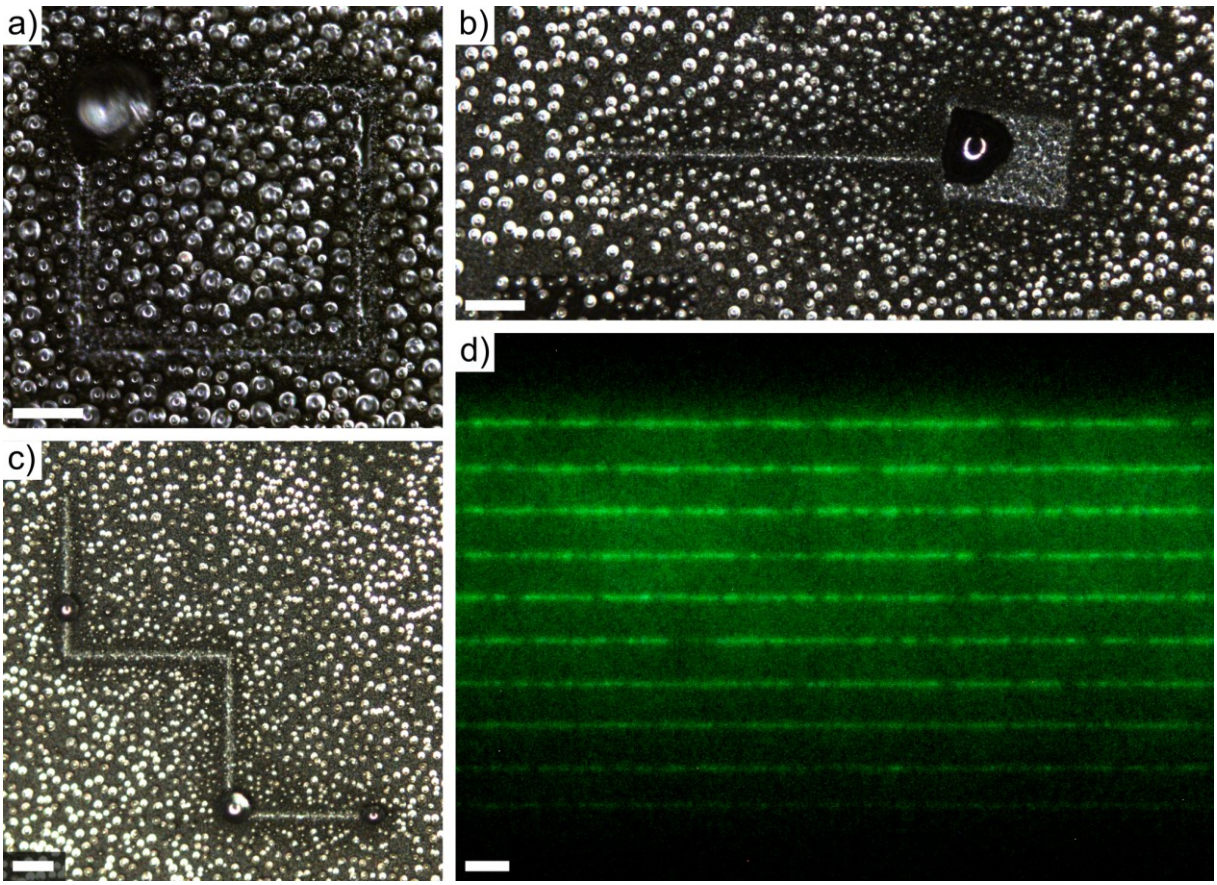

Figure 3. Condensation on fabricated patterns of different shapes. a-c) Optical micrographs of water condensation in ambient atmosphere on various patterns written in ESEM. Scale bars 50µm. d) Inverted optical microscope image of ten lines written in the ESEM. Scanning duration decreased in 0.1 s steps from 1 s for the topmost line to 0.1 s for the lowest line. The lines in the image are illuminated with blue light in the 450 – 489 nm wavelength range. Scale bar 10 µm.

Apart from black silicon coated with fluorinated parylene-C, other materials have also been considered (Figure S2, Supporting Information). Similar, increasing hydrophilicity effects

have been obtained for black silicon coated with a fluoropolymer, thermally hydrocarbonized porous silicon (THCPSi), and silicon dioxide. This shows that direct electron beam writing of wetting patterns in ESEM is not limited to fluorinated parylene-C.

To study the physical and chemical changes induced by the treatment, we used atomic force microscopy (AFM) and X-ray photoelectron spectroscopy (XPS) analyses. The AFM and XPS results, summarized in **Figure 4**, suggest that the radical change in the surface wetting properties of black silicon coated with parylene-C, when exposed to electron beam, is mainly due to modification of surface chemistry. No difference was observed in the surface topography in AFM, as shown in Figure 4b.

The XPS survey spectra from treated and non-treated areas of the sample are shown in Figure 4a. Similar backgrounds for F 1s, O 1s and C 1s signals[39,40] indicate uniform depth distributions for carbon, oxygen and fluorine on the non-treated area; that is uniform within the XPS analysis depth of 10 nm. Moreover, silica (Si 2p and Si 2s) backgrounds also indicate similar or at least non-covered depth distributions. Together with AFM data these results confirm existence of a uniform, fluorine rich organic open film of at least 10 nm in thickness on silicon substrate. Apart from the major compounds, chlorine and nitrogen were also detected with XPS. Nitrogen, however, was seen only on the treated area. In the treated area chlorine content was more than doubled (from 1.3 at.% to 3.1 at.%, see Table S1, Supporting Information) while the fluorine signal decreased by 24% (from 16.9 at.% to 12.5 at.%), indicating surface modification to the fluorocarbon film. Since the initial superhydrophobicity of the substrate is attributed to the topography of black silicon and the fluorinated parylene-C coating, reduction of the fluorinated fraction on the treated area leads to a decrease in hydrophobicity.

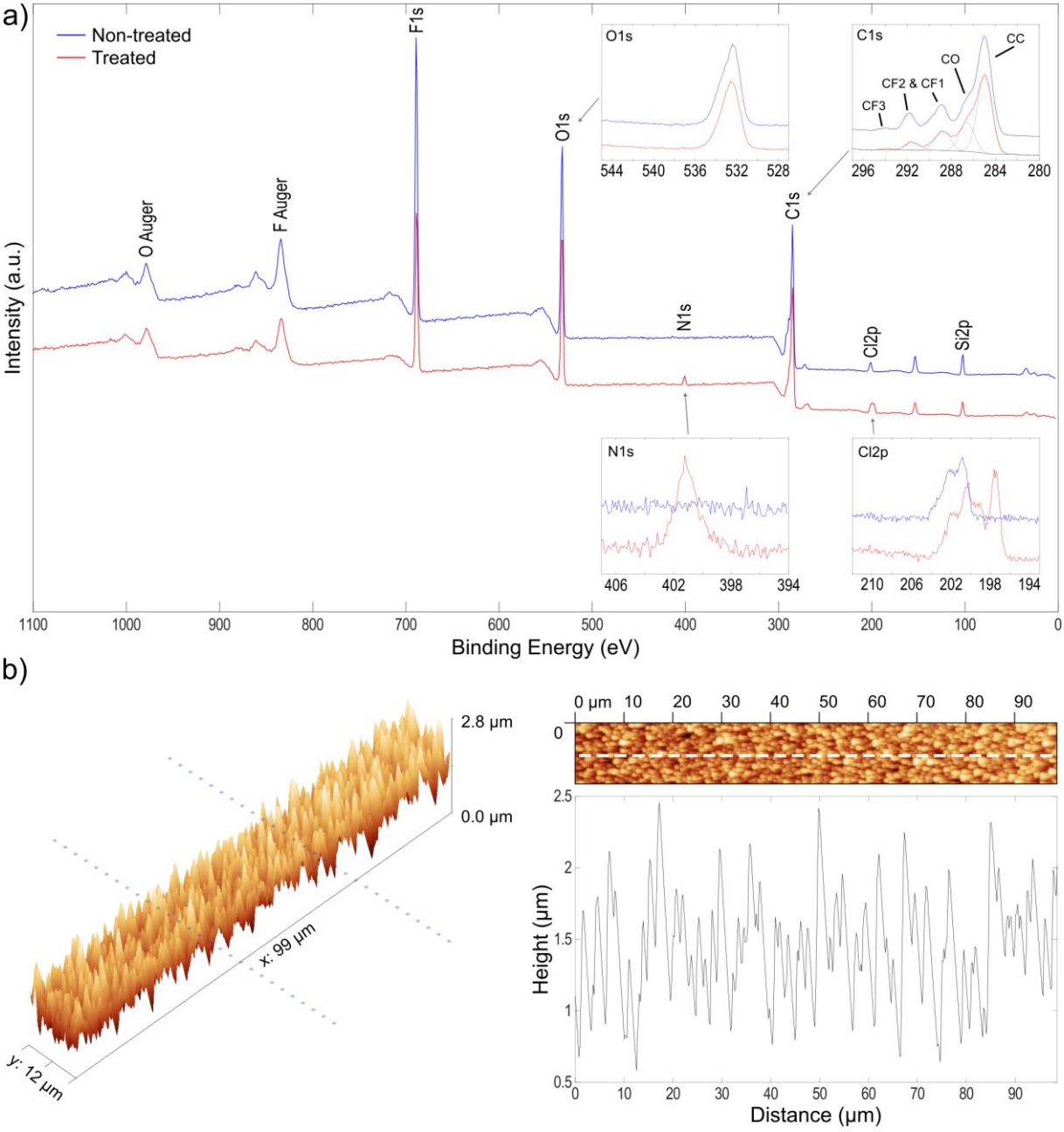

Figure 4. XPS and AFM results summary. a) Wide XPS survey spectrum for the treated area and non-treated background area; insets showing the high resolution XPS spectra for oxygen, carbon, nitrogen and chlorine. b) An AFM scan over the edge of the treated area, which is parallel to the y-axis between the two dotted lines; and cross-sectional profile along the white dashed line.

In the XPS high resolution data (insets in Figure 4a), the characteristic fluorocarbon components in C 1s confirm that the detected fluorine is bonded to carbon. Furthermore, oxygen and carbon chemistries were practically unaffected by the treatment. However, the high resolution XPS data reveals clear differences in chlorine chemistry (Cl 2p). The higher

binding energy component in chlorine, at around 200 eV, represents a chlorine compound containing oxygen and/or fluorine. This compound is present on both treated and non-treated areas of the substrate. The other peak, at 197 eV, represents organic chlorine without oxygen or fluorine neighbors, and this state was observed only on the treated area.

The other change revealed by XPS was nitrogen, which was detected only on the treated areas, as shown in Figure 4a, indicating the presence of nitrogen-containing, polar groups (–CN, =NH and $–NH_2$). These hydrophilic groups and the reduced fluorinated fraction turns the treated area to hydrophilic in nature, which is further enhanced to superhydrophilic by the roughness of the surface. It should be noted that while the treatment is carried out with water vapor as the imaging gas, it is preceded by sample navigation in nitrogen in order to avoid altering the surface during navigation. Therefore, residual nitrogen remains in the chamber. The fact that carrying out the treatment in pure nitrogen does not induce the superhydrophobic to superhydrophilic transition suggests that nitrogen alone is not reactive enough. However, in the presence of reactive species ionized from the water vapor, such as [H], [O], [OH],[41] nitrogen can interact with the surface. In this sense, the mechanism is related to air, nitrogen and oxygen plasma treatments, which have been used to turn superhydrophobic surfaces superhydrophilic.[42–45]

It is also worth noting that the XPS analysis did not show noticeable changes in oxygen content of the surface. The effect of the electron beam through water vapor is therefore different from oxygen plasma treatment, which is well known to increase the hydrophilicity of parylene-C.[46–49] Furthermore, the effect of an oxygen plasma treatment tends to weaken in a few days as the parylene-C film recovers some of its hydrophobicity.[50] In our method the patterns retain superhydrophilicity even after a year, making the treatment practically permanent.

The emission of bright light of the treated areas under UV irradiation is attributed to the autofluorescence of parylene-C. In an earlier study, Lu et al. reported strong fluorescence in the visible light range in parylene-C during short-time (a few minutes) UV illumination,[51] caused by dehydrogenation of the carbon chain and/or aromatic ring. In our case, the treated area is likely to contain more hydrogen bound to the polymer structure, because it has less fluorine occupying the carbon sites compared to the background. The treated areas also have hydrogen bound in the hydrophilic polar groups (=NH, $–NH_2$), leading to stronger dehydrogenation and thus greater fluorescence intensity.

In summary, we have presented a new, direct electron beam writing method for maskless, programmable wettability patterning in ESEM. We produced superhydrophilic features on superhydrophobic black silicon coated with fluorinated parylene-C, and observed wettability modification effects on other materials as well. The method can be used to write features down to one micrometer in size, which is comparable to the feature size of the coated black silicon surface. This is the limit where the surface can be considered homogeneous for the purposes of wetting and condensation.

Our work has important implications for micro and nanoscale wetting studies in ESEM, which has been used for e.g. observing the wetting dynamics of evaporation-condensation on superhydrophobic surfaces,[52,53] the fine structure of the triple line and Cassie-Wenzel wetting transition,[54] growth and shedding of condensing droplets,[55] microdroplet growth mechanism during water condensation on superhydrophobic surfaces,[56] and multidrop coalescence effects during condensation on superhydrophobic surfaces.[57] Our results indicate that when ESEM is used in high-resolution wetting studies, the reactive species ionized by the

electron beam may modify the wetting properties of the sample surface during observation, distorting the results.

Experimental Section

Superhydrophobic surface synthesis: Preparation of the parylene-C coated black silicon surface was performed on a single side polished, 100 mm diameter, 500 µm thick silicon (100) wafer (Siegert Wafer GmbH, Germany). Black silicon was formed in a cryogenic, inductively coupled plasma reactive ion etcher (ICP-RIE; Plasmalab System 100, Oxford Instruments, UK) for 7 min using experimentally optimized parameters: 40 sccm SF_6 flow, 18 sccm O_2 flow, 6 W forward power, 1000 W ICP power, -110 °C temperature, 10 mTorr pressure, with helium backside cooling. In the next step, approximately 250 nm of parylene-C was deposited on top of the black silicon wafer using a parylene deposition system (Labcoter 2 PDS 2010, Specialty Coating Systems, USA). The thickness of the parylene-C film was estimated by coating a plain silicon wafer using the same parameters and measuring the thickness using an optical ellipsometer (SD 2300, PLASMOS GmbH, Germany). Finally, the parylene-C coated black silicon substrate was fluorinated in a reactive ion etcher (RIE; PlasmaLab 80 Plus, Oxford Instruments, UK) for 1 min using 100 sccm SF_6 flow, 100 W forward power, and 20 mTorr pressure, resulting in a 200 nm parylene-C thickness.

Electron beam treatment: The fluorinated black silicon/parylene-C surface was modified by local exposure to electron beam in an environmental scanning electron microscope (ESEM; EVO HD-15-LS, Carl Zeiss AG, Germany) in the presence of water vapor in the chamber. Before each treatment, sample navigation was performed in 200 Pa nitrogen atmosphere and the sample stage at room temperature. After sample navigation, nitrogen was replaced with 625 Pa water vapor, and the sample stage was cooled down to 1.5 °C to reach 92 % relative humidity near the sample surface. The temperature of the sample stage was allowed to settle

for 15 min. Patterns were created by either holding the beam at one spot and scanning the sample stage, or holding the sample still and scanning the beam over the sample. The acceleration voltage was 30 kV, working distance 4.5 mm, beam current 5 nA, and treatment time was chosen based on the size and type of the target pattern, varying from 1 s to 20 min. The effect and selection of treatment parameters are discussed in more detail in the Supporting Information.

Characterization: Surface topography of the treated areas and the background was measured using an atomic force microscope (AFM; Dimension 5000, Veeco Instruments, USA) in tapping mode.

X-ray photoelectron spectroscopy (XPS) analysis was performed using an X-ray photoelectron spectrometer (AXIS Ultra, Kratos Analytical, UK), with monochromatic Al Kα irradiation at low power setting (100 W), under neutralization and with nominal analysis area of 400 × 800 μm^2. A fresh piece of 100% cellulose was measured with each sample batch, as an in-situ reference.[58] Elemental surface compositions were determined from low resolution survey spectra (1 eV step, 80 eV CAE), while the high resolution regional data of C 1s, O 1s, Cl 2p and N 1s were used in detailed chemical analysis (0.1 eV step, 20 eV CAE). The aliphatic component in high resolution C 1s peak at 285.0 eV was utilized as the binding energy reference for all spectra.[59] The data analysis was performed with CasaXPS.

Condensation tests: Condensation tests were carried out in ambient air, under optical microscope (BX-60, Olympus Corporation, Japan). The samples were placed on a block of aluminum that was cooled down or heated up from the back side using a Peltier element. Relative humidity in the room-temperature laboratory was 40%, leading to condensation at 7 °C temperature of the sample surface. The condensation-evaporation cycles were recorded with a CCD camera (B1922C, Imperx Inc., USA) attached to the optical microscope.

Optical microscopy: To make the patterns visible under optical microscope, ultraviolet light from a UV spot light source (BlueWave 50, Dymax Corporation, USA) was directed at the patterns from a distance of a few centimeters. Higher magnification images for visualization and measurement of the smallest pattern linewidth were obtained using an inverted microscope (Axio Vert. A1, Carl Zeiss AG, Germany) equipped with a fluorescence light source (X-Cite 120Q, Lumen Dynamics, Canada). A filter was applied that lets through blue light in the 450 – 489nm range. The images were captured by a DSLR camera (EOS 550D, Canon Inc., Japan).

Contact angle (CA) measurements: Contact angles were measured on both the modified areas and the background using the dynamic sessile drop method, where the volume of a sessile water drop in touch with the surface is increased and decreased to obtain the advancing and receding contact angles, respectively. The measurements were carried out using a custom built set-up equipped with sub-µm precision motorized stages for XYZ positioning (M-404.8PD, M-122.2PD and M-111.1PD, Physik Instrumente GmbH, Germany), a syringe pump for dispensing water with 1 nl resolution (Cavro XP3000+, Tecan, Switzerland). The wetting contrast of the exposed areas to the background was also demonstrated by shooting nanoliter-sized water droplets at the surface using a non-contact microdispenser (PicPIP, GeSiM mbH, Germany). The droplet impacts on the surface were recorded using a high-speed digital camera (Phantom Miro LC310, Vision Research, USA) equipped with a macro photo lens (MP-E 65mm, Canon Inc., Japan).

Supporting Information
Supporting Information is available from the Wiley Online Library or from the author.

Acknowledgements
This research was supported by the Aalto ELEC Doctoral School, the Aalto Energy Efficiency Programme (project MOPPI, 2012-2016) and the Academy of Finland's Centres of Excellence Programme (HYBER, 2014-2019). We also acknowledge the provision of facilities and technical support by Aalto University at Micronova Nanofabrication Centre, and the use of Aalto University Bioeconomy Facilities. The authors are grateful to Dr. Joe Campbell for performing XPS experiments, to Dr. Veikko Sariola for comments on the manuscript, and to Dr. Hélder Santos (Helsinki University) for providing THCPSi samples.

Received: ((will be filled in by the editorial staff))
Revised: ((will be filled in by the editorial staff))
Published online: ((will be filled in by the editorial staff))

[1] A. R. Parker, C. R. Lawrence, *Nature* **2001**, *414*, 33.

[2] H.-J. Jin, D. L. Kaplan, *Nature* **2003**, *424*, 1057.

[3] X. Yao, Y. Song, L. Jiang, *Adv. Mater.* **2011**, *23*, 719.

[4] E. Ueda, P. A. Levkin, *Adv. Mater.* **2013**, *25*, 1234.

[5] L. Zhai, M. C. Berg, F. Ç. Cebeci, Y. Kim, J. M. Milwid, M. F. Rubner, R. E. Cohen, *Nano Lett.* **2006**, *6*, 1213.

[6] A. R. Betz, J. Jenkins, C.-J. "CJ" Kim, D. Attinger, *Int. J. Heat Mass Transf.* **2013**, *57*, 733.

[7] V. Sariola, M. Jääskeläinen, Q. Zhou, *IEEE Trans. Robot.* **2010**, *26*, 965.

[8] D. Nepal, M. S. Onses, K. Park, M. Jespersen, C. J. Thode, P. F. Nealey, R. A. Vaia, *ACS Nano* **2012**, *6*, 5693.

[9] D. K. Gramotnev, S. I. Bozhevolnyi, *Nat. Photonics* **2010**, *4*, 83.

[10] S. Xing, R. S. Harake, T. Pan, *Lab Chip* **2011**, *11*, 3642.

[11] V. Liimatainen, V. Sariola, Q. Zhou, *Adv. Mater.* **2013**, *25*, 2275.

[12] F. L. Geyer, E. Ueda, U. Liebel, N. Grau, P. A. Levkin, *Angew. Chemie Int. Ed.* **2011**, *50*, 8424.

[13] S. Friebel, J. Aizenberg, S. Abad, P. Wiltzius, *Appl. Phys. Lett.* **2000**, *77*, 2406.

[14] Y.-L. Yang, C.-C. Hsu, T.-L. Chang, L.-S. Kuo, P.-H. Chen, *Appl. Surf. Sci.* **2010**, *256*, 3683.

[15] E. Martines, K. Seunarine, H. Morgan, N. Gadegaard, C. D. W. Wilkinson, M. O. Riehle, *Nano Lett.* **2005**, *5*, 2097.

[16] B. M. Wei, L. Fang, J. Lee, S. Somu, X. Xiong, C. Barry, A. Busnaina, J. Mead, *Adv. Mater.* **2009**, *21*, 794.

[17] W. Chang, M. Choi, J. Kim, S. Cho, K. Whang, *Appl. Surf. Sci.* **2005**, *240*, 296.

[18] Y. Lin, M. H. Hong, W. J. Wang, Z. B. Wang, G. X. Chen, Q. Xie, L. S. Tan, T. C. Chong, *Sensors Actuators A Phys.* **2007**, *133*, 311.

[19] U. Manna, A. H. Broderick, D. M. Lynn, *Adv. Mater.* **2012**, *24*, 4291.

[20] J. Wu, H. Li, X. Qi, Q. He, B. Xu, H. Zhang, *Small* **2014**, *10*, 2239.

[21] V. Zorba, L. Persano, D. Pisignano, a Athanassiou, E. Stratakis, R. Cingolani, P. Tzanetakis, C. Fotakis, *Nanotechnology* **2006**, *17*, 3234.

[22] A.-M. Kietzig, S. G. Hatzikiriakos, P. Englezos, *Langmuir* **2009**, *25*, 4821.

[23] D. Losic, J. G. Shapter, J. J. Gooding, *Langmuir* **2001**, *17*, 3307.

[24] I. V. Vasiljeva, S. V. Mjakin, A. V. Makarov, A. N. Krasovsky, A. V. Varlamov, *Appl. Surf. Sci.* **2006**, *252*, 8768.

[25] M. L. Cairns, G. R. Dickson, J. F. Orr, D. Farrar, C. Hardacre, J. Sa, P. Lemoine, M. Z. Mughal, F. J. Buchanan, *J. Biomed. Mater. Res. - Part A* **2012**, *100 A*, 2223.

[26] P. Sen Majumder, A. K. Bhowmick, *Radiat. Phys. Chem.* **1999**, *53*, 63.

[27] M. S. Ibrahim, K. M. El Salmawi, S. M. Ibrahim, *Appl. Surf. Sci.* **2005**, *241*, 309.

[28] D. Aronov, G. Rosenman, *Surf. Sci.* **2007**, *601*, 5042.

[29] I. Torchinsky, G. Rosenman, *Nanoscale Res. Lett.* **2009**, *4*, 1209.

[30] X. Chen, J. Wu, R. Ma, M. Hua, N. Koratkar, S. Yao, Z. Wang, *Adv. Funct. Mater.* **2011**, *21*, 4617.

[31] C. Dorrer, J. Rühe, *Adv. Mater.* **2008**, *20*, 159.

[32] N. M. Suni, M. Haapala, A. Mäkinen, L. Sainiemi, S. Franssila, E. Färm, E. Puukilainen, M. Ritala, R. Kostiainen, *Angew. Chemie - Int. Ed.* **2008**, *47*, 7442.

[33] B. Chang, A. Shah, I. Routa, H. Lipsanen, Q. Zhou, *Appl. Phys. Lett.* **2012**, *101*.

[34] A. R. Betz, J. R. Jenkins, C. J. Kim, D. Attinger, *Proc. IEEE Int. Conf. Micro Electro Mech. Syst.* **2011**, 1193.

[35] I. Routa, B. Chang, A. Shah, Q. Zhou, *J. Microelectromechanical Syst.* **2014**, *23*, 819.

[36] V. Jokinen, L. Sainiemi, S. Franssila, *Adv. Mater.* **2008**, *20*, 3453.

[37] S. Boduroglu, M. Cetinkaya, W. J. Dressick, A. Singh, M. C. Demirel, *Langmuir* **2007**, *23*, 11391.

[38] K. G. Pruden, K. Sinclair, S. Beaudoin, *J. Polym. Sci. Part A Polym. Chem.* **2003**, *41*, 1486.

[39] S. Tougaard, *Surf. Interface Anal.* **1998**, *26*, 249.

[40] L.-S. Johansson, J. Campbell, K. Koljonen, M. Kleen, J. Buchert, *Surf. Interface Anal.* **2004**, *36*, 706.

[41] Y. Itikawa, *J. Phys. Chem. Ref. Data* **2005**, *34*, 1.

[42] E. Bormashenko, R. Grynyov, *Colloids Surfaces B Biointerfaces* **2012**, *92*, 367.

[43] A. Pakdel, Y. Bando, D. Golberg, *ACS Nano* **2014**, *8*, 10631.

[44] A. Chaudhary, H. C. Barshilia, *J. Phys. Chem. C* **2011**, *115*, 18213.

[45] X. Zhu, Z. Zhang, X. Men, J. Yang, X. Xu, *ACS Appl. Mater. Interfaces* **2010**, *2*, 3636.

[46] J. S. Song, S. Lee, S. H. S. Jung, G. C. Cha, M. S. Mun, *J. Appl. Polym. Sci.* **2009**, *112*, 3677.

[47] X. P. Bi, N. L. Ward, B. P. Crum, W. Li, in *2012 7th IEEE Int. Conf. Nano/Micro Eng. Mol. Syst. NEMS 2012*, **2012**, pp. 222–225.

[48] M. Gołda, M. Brzychczy-Włoch, M. Faryna, K. Engvall, A. Kotarba, *Mater. Sci. Eng. C* **2013**, *33*, 4221.

[49] T. Y. Chang, V. G. Yadav, S. De Leo, A. Mohedas, B. Rajalingam, C. L. Chen, S. Selvarasah, M. R. Dokmeci, A. Khademhosseini, *Langmuir* **2007**, *23*, 11718.

[50] T. Trantidou, T. Prodromakis, C. Toumazou, *Appl. Surf. Sci.* **2012**, *261*, 43.

[51] B. Lu, S. Zheng, B. Q. Quach, Y.-C. Tai, *Lab Chip* **2010**, *10*, 1826.

[52] M. Nosonovsky, B. Bhushan, *Nano Lett.* **2007**, *7*, 2633.

[53] Y. C. Jung, B. Bhushan, *J. Microsc.* **2008**, *229*, 127.

[54] E. Bormashenko, Y. Bormashenko, T. Stein, G. Whyman, R. Pogreb, Z. Barkay, *Langmuir* **2007**, *23*, 4378.

[55] S. Anand, A. T. Paxson, R. Dhiman, J. D. Smith, K. K. Varanasi, *ACS Nano* **2012**, *6*, 10122.

[56] K. Rykaczewski, *Langmuir* **2012**, *28*, 7720.

[57] K. Rykaczewski, A. T. Paxson, S. Anand, X. Chen, Z. Wang, K. K. Varanasi, *Langmuir* **2013**, *29*, 881.

[58] L.-S. Johansson, J. M. Campbell, *Surf. Interface Anal.* **2004**, *36*, 1018.

[59] G. Beamson, D. Briggs, *High Resolution XPS of Organic Polymers, The Scienta ESCA 300 Database John Wiley & Sons*, **1992**.

A maskless and programmable direct electron beam writing method is reported for making high-precision superhydrophilic-superhydrophobic wetting patterns with 152° contact angle contrast using an environmental scanning electron microscope (ESEM). The smallest linewidth achieved is below 1 µm. Beyond precision patterning, effects of the local plasma induced by the electron beam are shown, which may influence a variety of microscopic wetting studies in ESEM.

wettability patterning, electron beam modification, ESEM, superhydrophobicity, superhydrophilicity

V. Liimatainen, A. Shah, L-S. Johansson, Q. Zhou*

Maskless, High-Precision, Persistent and Extreme Wetting-Contrast Patterning in an Environmental Scanning Electron Microscope